IEEE Radar Conference 2010

Spatially-Varying Calibration of Along-Track Monopulse Synthetic Aperture Radar Imagery for Ground Moving Target Indication and Tracking

Uttam Majumder, Mehrdad Soumekh, Michael Minardi, John Kirk

Air Force Research Laboratory (AFRL/RYAS)

Soumekh Consulting

Goleta Star LLC

Public Release Numbers:
WPAFB-08-1102; 88 ABW-09-0181; 88 ABW-09-1197

Outline

1. Objectives
2. Multiple Moving Targets Detection
3. Multiple Moving Targets Association and Tracking
4. Ground Plane Geolocation
5. Summary

1. Objectives

1. ***Detect*** multiple moving targets in a heavy clutter (urban) environment using a single-pass with one or more along-track receivers and/or multiple-pass SAR
2. ***Associate*** detections in ***subaperture*** SAR imagery to identify the radial-range and Doppler tracks of each target
3. ***Geolocate*** each detected and tracked moving target using its subaperture radial-range and Doppler data with or without information on network of roads

2.1 Multiple Moving Targets Detection: Possible Databases

- SAR-MTI is constructed using a 2D adaptive change detection algorithm
- We have tested three types of databases (options) to form ***Reference*** and ***Test*** images.
- The option that is presented is this paper is:
  - Subaperture monostatic and along-track bistatic (DPCA) monopulse SAR data from a single pass (coherent change detection)

*Why **subaperture**-based processing?*

- For an IR or visible camera, a moving target appears: a) slightly blurred but still detectable via change detection in an image sequence; & b) around its true spatial coordinates (on camera’s focal plane)
- In a full-aperture (-resolution) SAR image: a) to say a moving *vehicle* signature appears blurred is an understatement; & b) the mover signature would be Doppler-shifted
- In a subaperture SAR image, a mover would be more localized for detection purposes though still Doppler-shifted

2.2a Adaptive Filtering for Reference-Test Image Calibration

- 2D Adaptive filtering method (called Signal Subspace Processing, SSP) compensates for
  1. Unknown variations of the electronics, antennas, etc. of the two SAR databases
  2. Spatial warping in the test and reference imagery due to unknown INS errors and/or unknown variations in target area height
- Interferometric (phase only) processing for change detection could also benefit from adaptively calibrated imagery

2.2b Local SSP

- A realistic miscalibration model for the two receiver channels is based on the fact that the ***filter is spatially-varying***. In this case, the relationship between the test and reference images can be expressed via the following:

$$\hat{f}_{RT}(x,y) = \int f_R(x-u, y-v)\ h_{xy}(u,v)\, du\, dv$$

where in this model the filter $h_{xy}(u,v)$ varies with the spatial coordinates (x,y).

- While the above model is a more suitable one, however, it is computationally prohibitive to implement the LMS or SSP method for this scenario.
- A practical alternative is to assume that the filter is approximately spatially-invariant within a small area in the spatial domain.
- In this case, we can divide the imaging scene into subpatches within which the filter can be approximated to be spatially-invariant.

LSSP

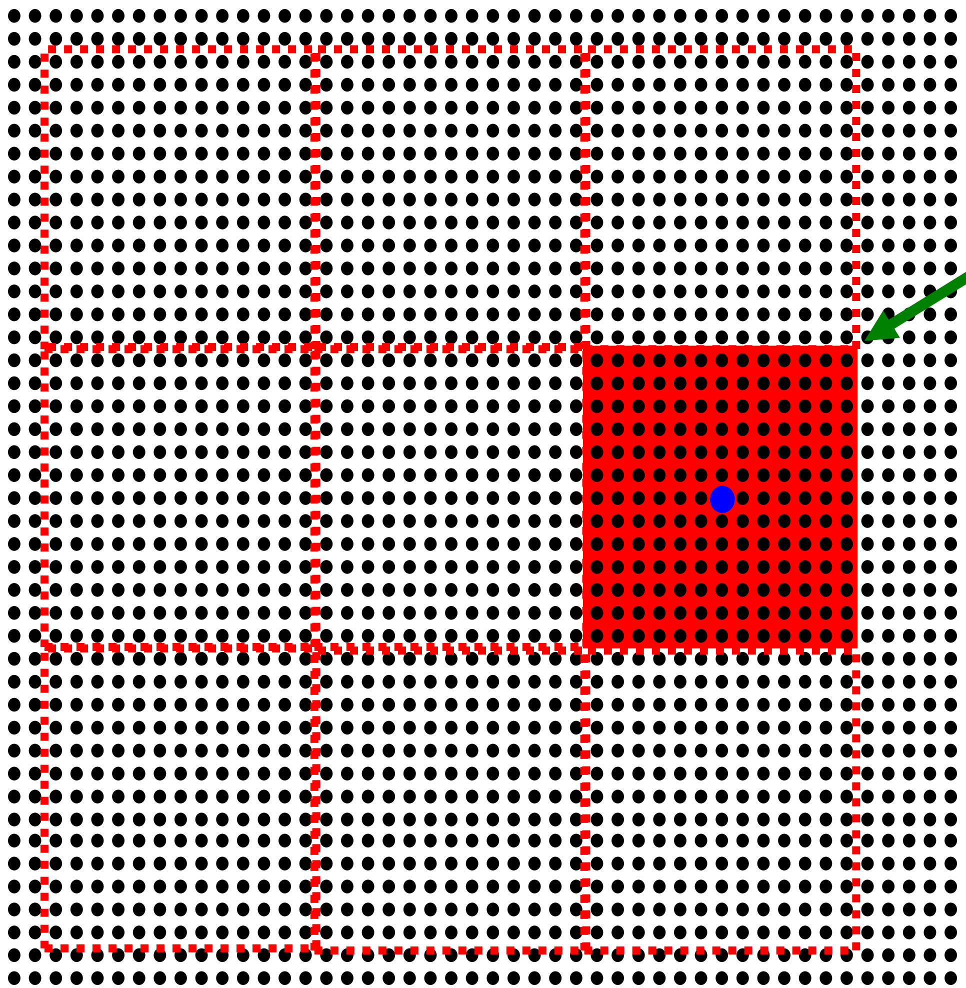

Subpatch Number i is centered at (xi, yi)

Solution of 2D Adaptive Filter is Assigned to This Grid Point

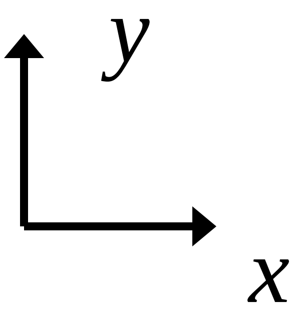

2.2c Global SSP

- After the calibration filter is estimated for each subpatch, an approach that we call ***Global Signal Subspace Processing*** (GSSP) is used to estimate the original spatially-varying filter

- Available samples of 2D adaptive filter for the subpatches $h_\ell(u,v)$ are at the grid point (x_ℓ, y_ℓ); these are shown as blue dots.
- For every (u,v) (that is the 2D filter domain), the values of the 2D spatially-varying filter $h_{xy}(u,v)$ are interpolated on the original image grid in the spatial domain (x,y) (black dots) from the available filter samples $h_\ell(u,v)$ at the grid points (x_ℓ, y_ℓ) (blue dots).

GSSP

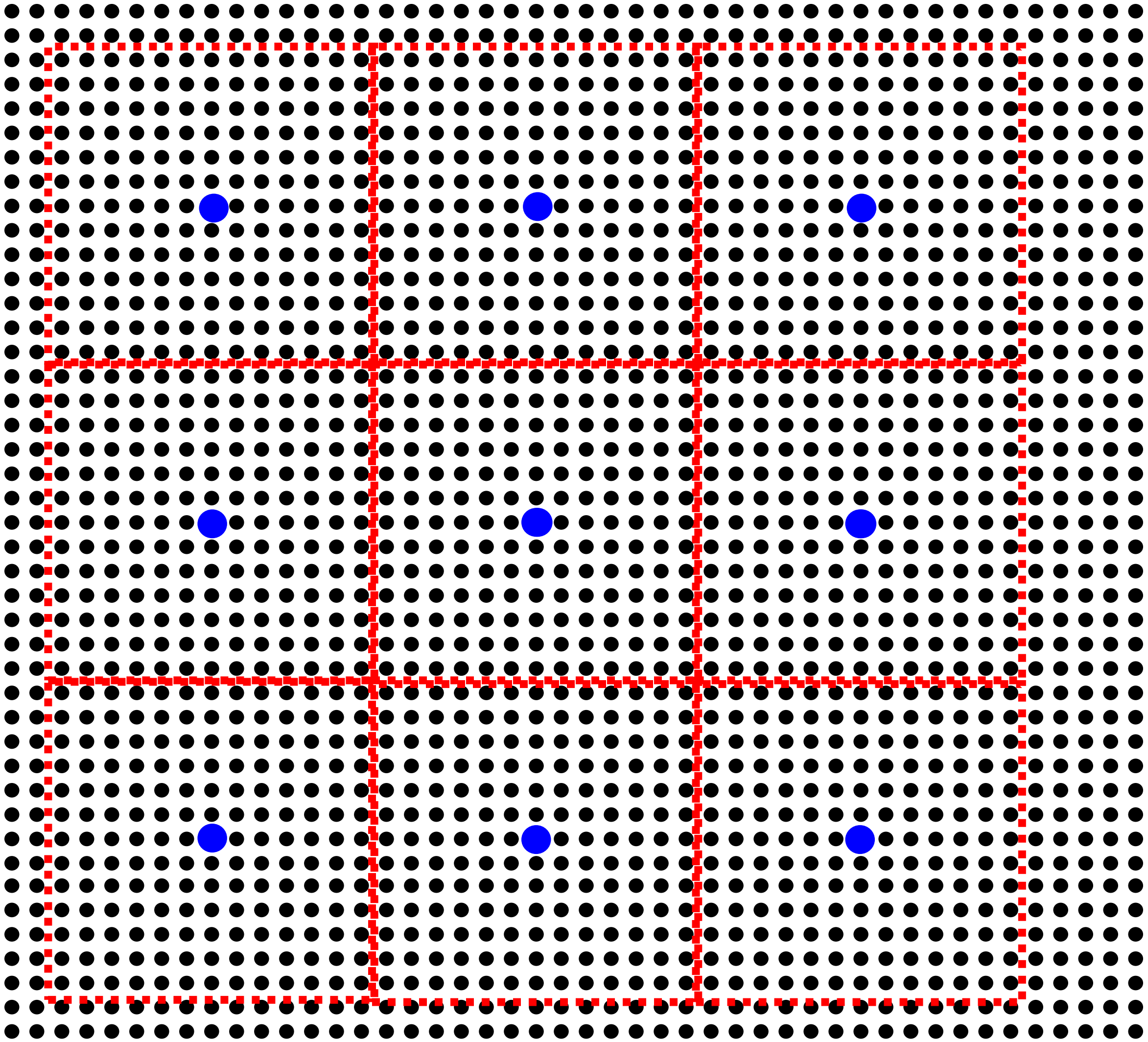

Available Samples are in Blue

Interpolated Points are in Black

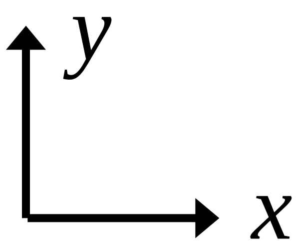

2.3 SAR-MTI Using Monostatic and Along-Track Bistatic Monopulse Configuration (DPCA-MTI, Option 1)

Imaging System Geometry: Top View

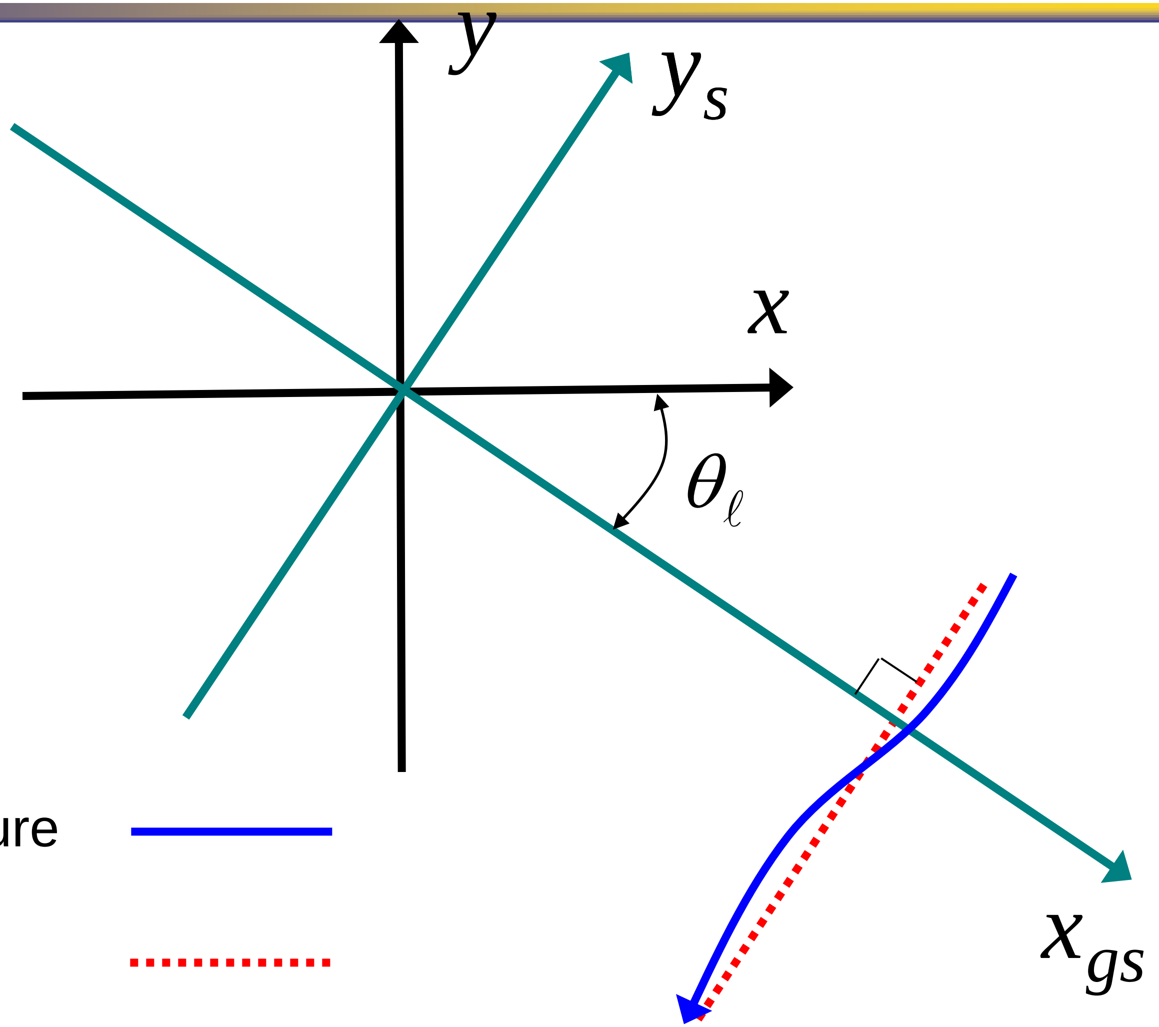

Nonlinear Subaperture

Synthesized Linear Subaperture

Coherent Clutter Suppression Using GSSP on Slant-Plane

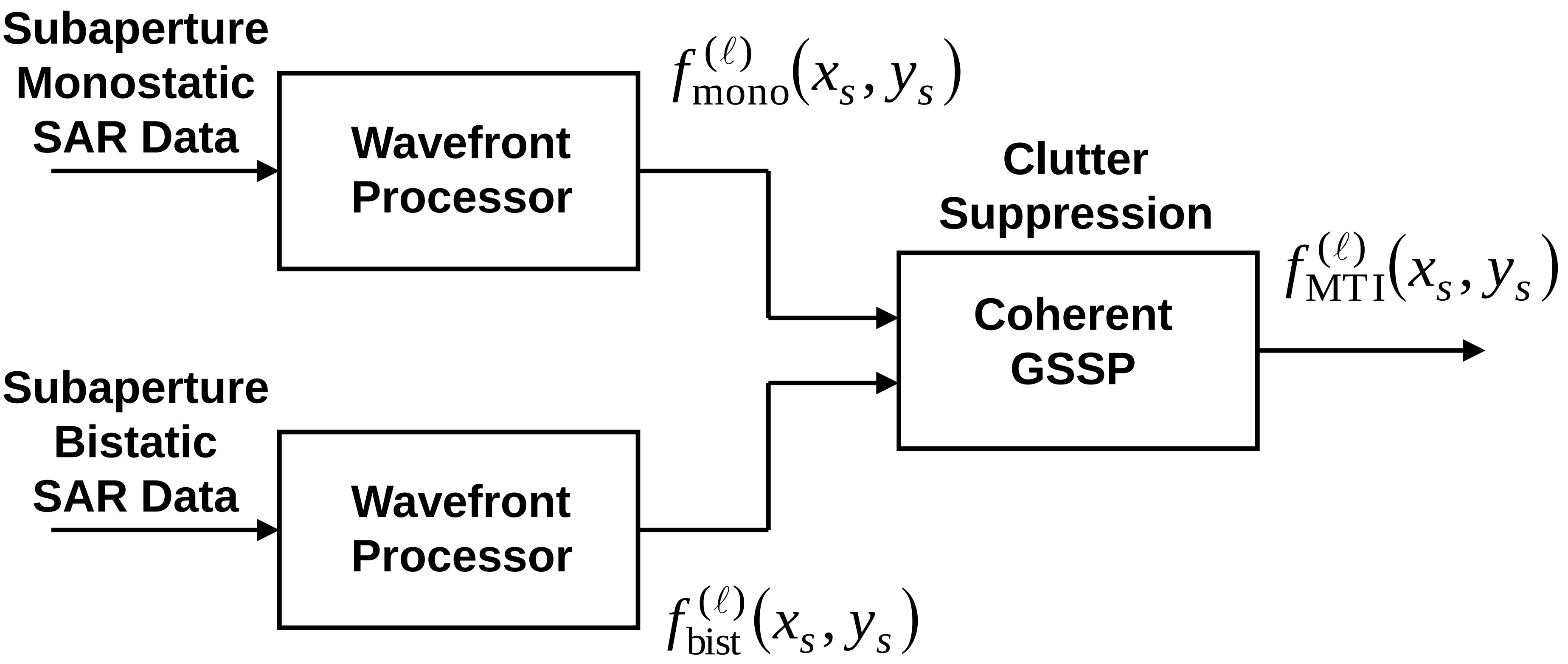

UTM Transform and Residual Clutter Suppression on Ground Plane

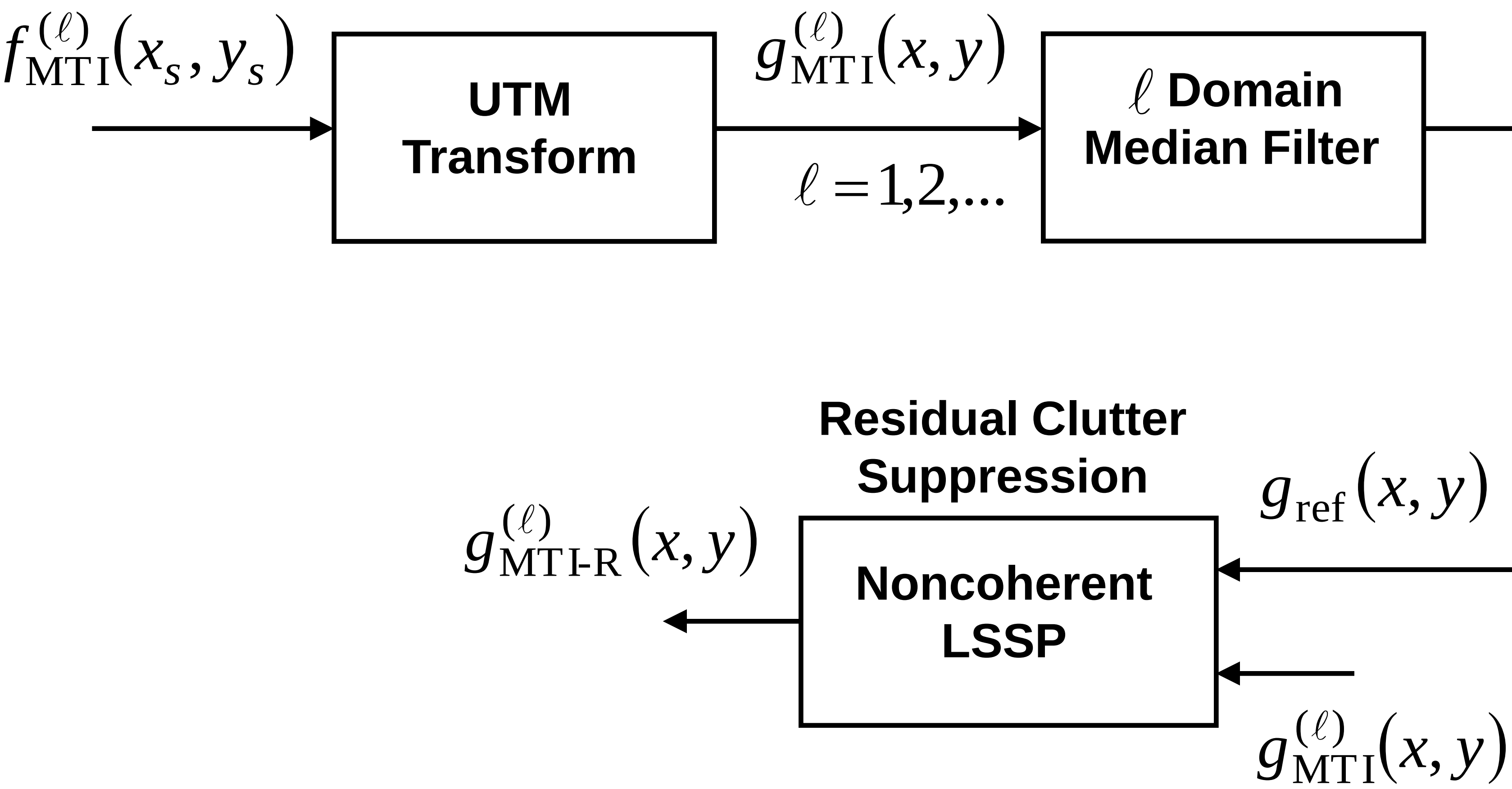

Results with Gotcha SAR Data

Subaperture Processing:
1024 PRIs (.5 sec) per Subaperture
512-PRI Overlapping Subapertures
(.25 sec updating)

Imaging System Geometry: Subapertures 1-40

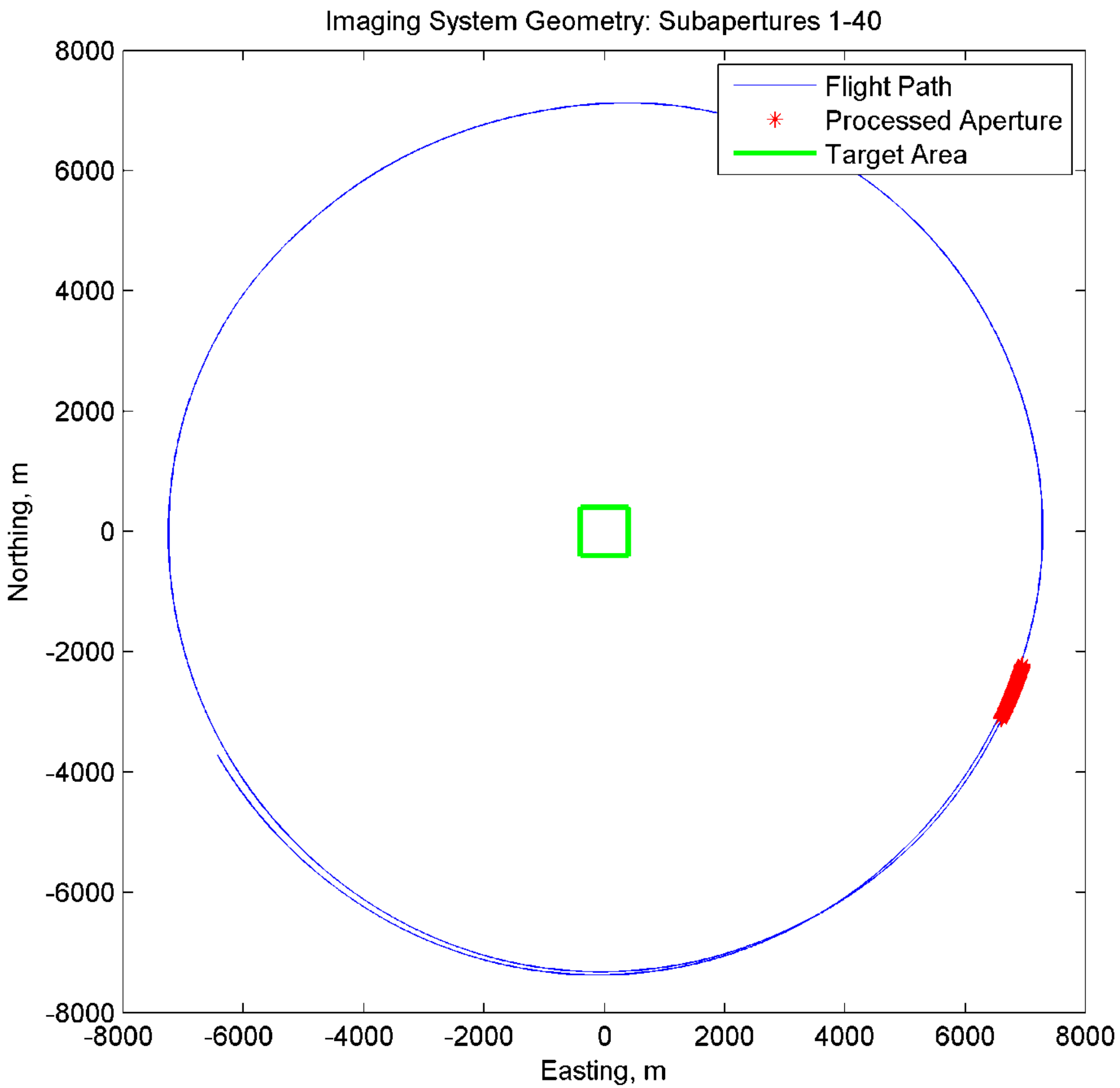

Full-Aperture Reconstruction

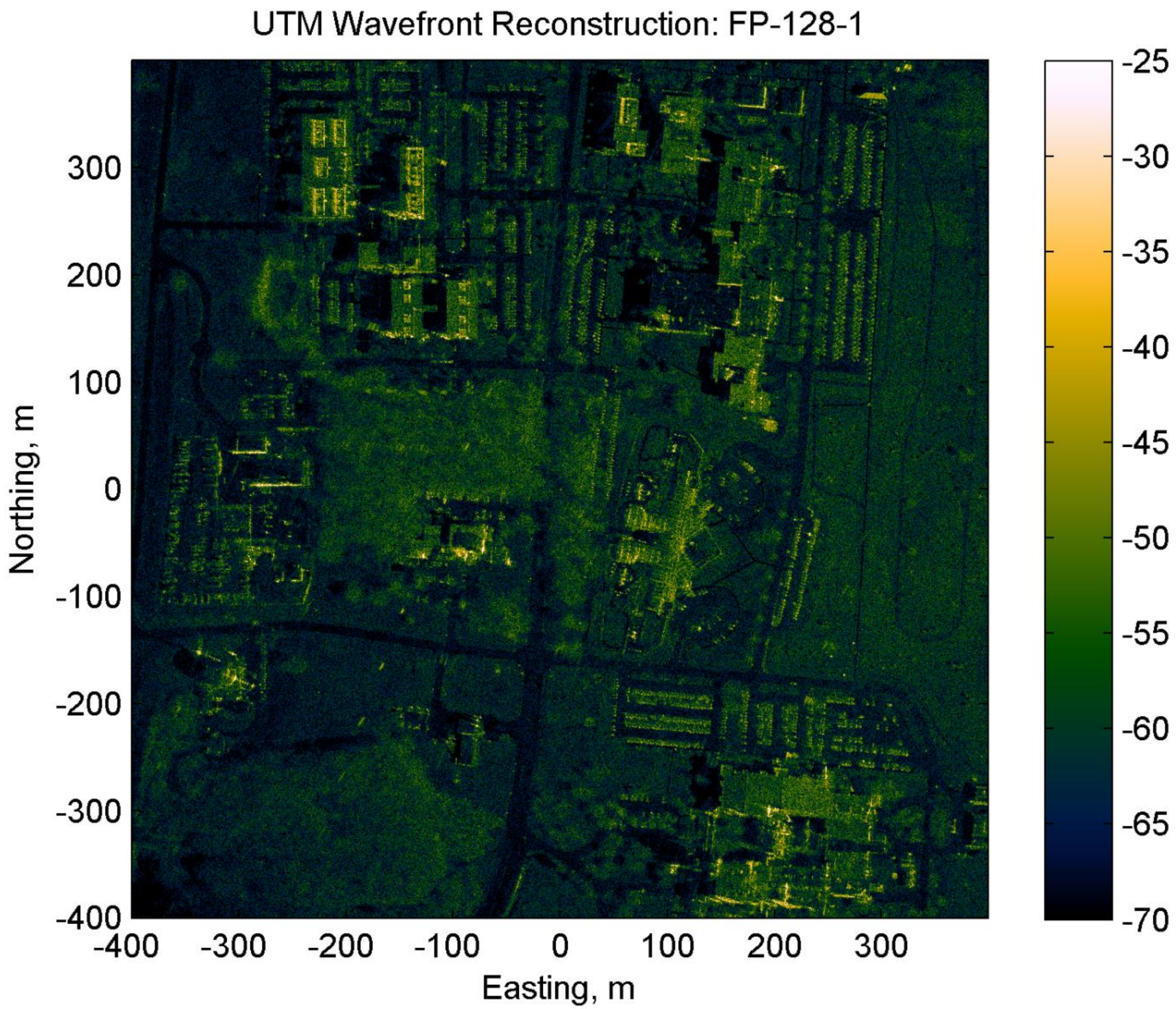

Subaperture Reconstruction

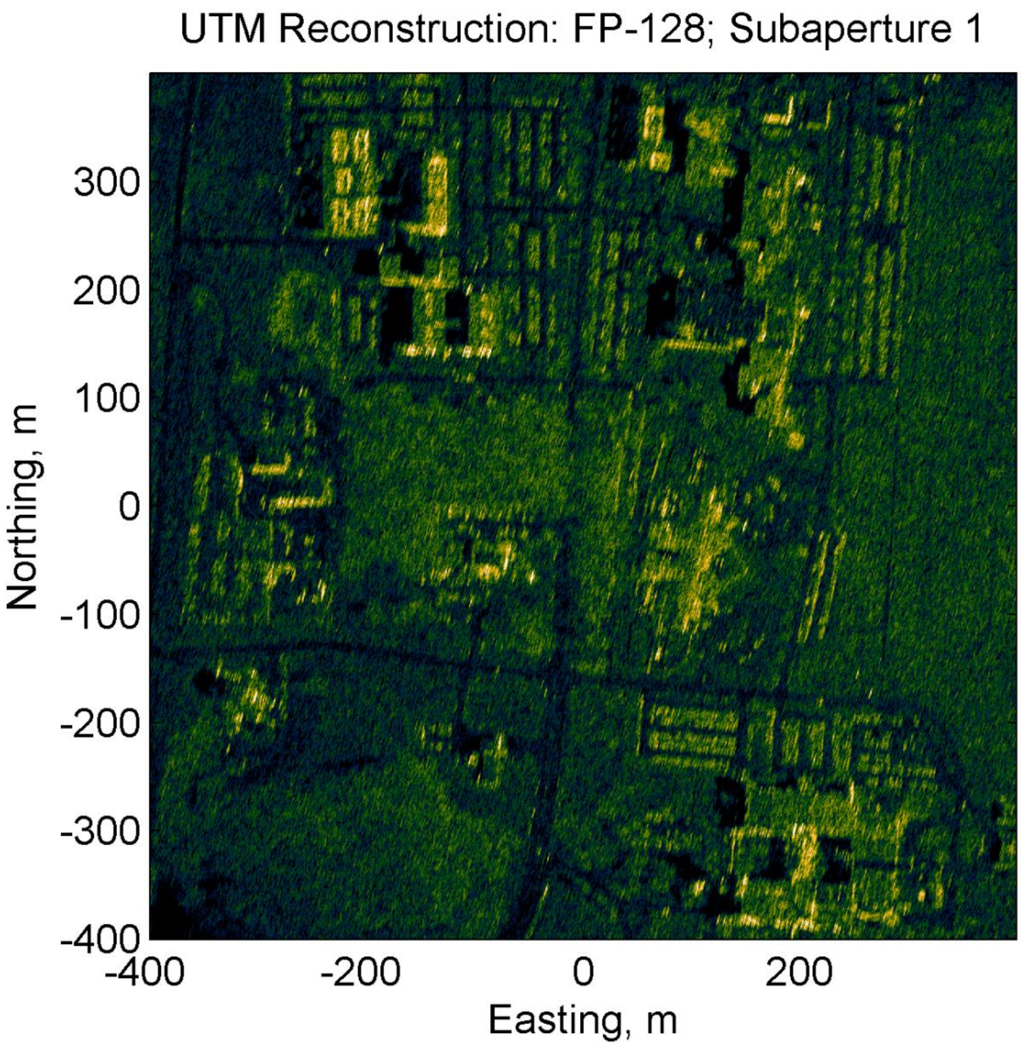

MTI Detections:
Coherent Single Pass
Dual Receivers

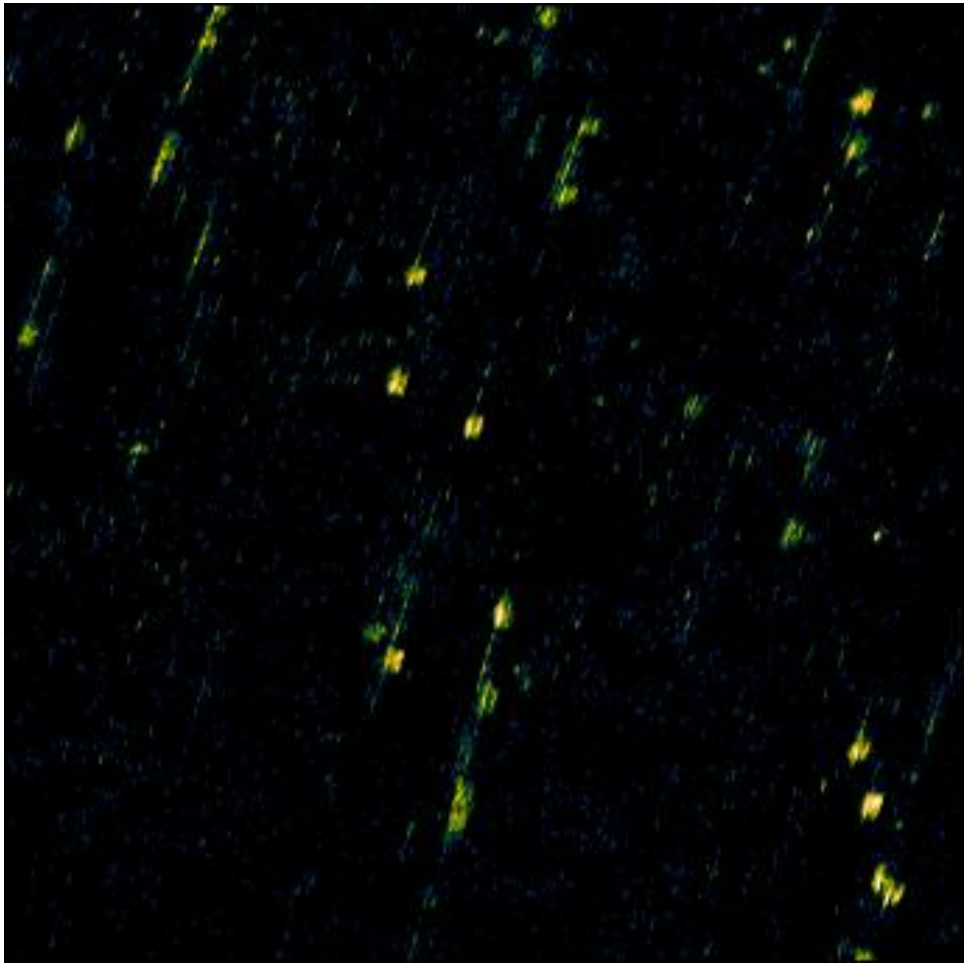

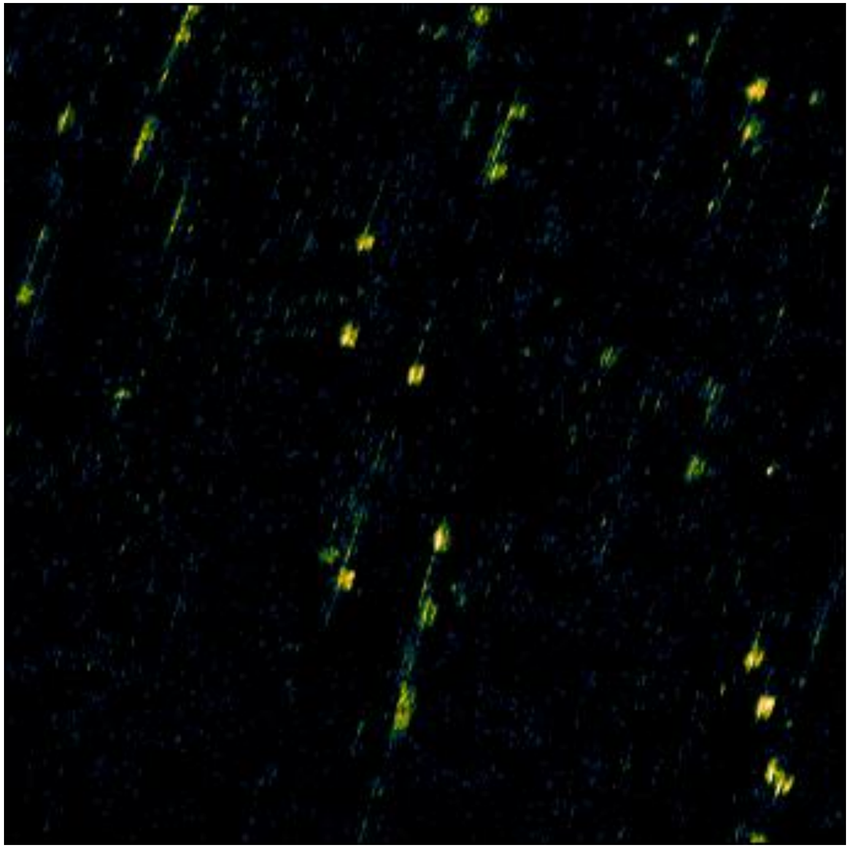

3. Multiple Moving Targets Association and Tracking

- An algorithm that uses linear prediction to associate MTI hits in IR and visible camera imagery is the basis of our approach for SAR-MTI tracking problem
- This approach is used on processing the MTI hits on the ground plane SAR image
- The algorithm could exploit our analytical study of SAR geolocation based on radial-range and angular-Doppler shift information of MTI hits (that is discussed later)

Tracks of Four Detected Moving Targets

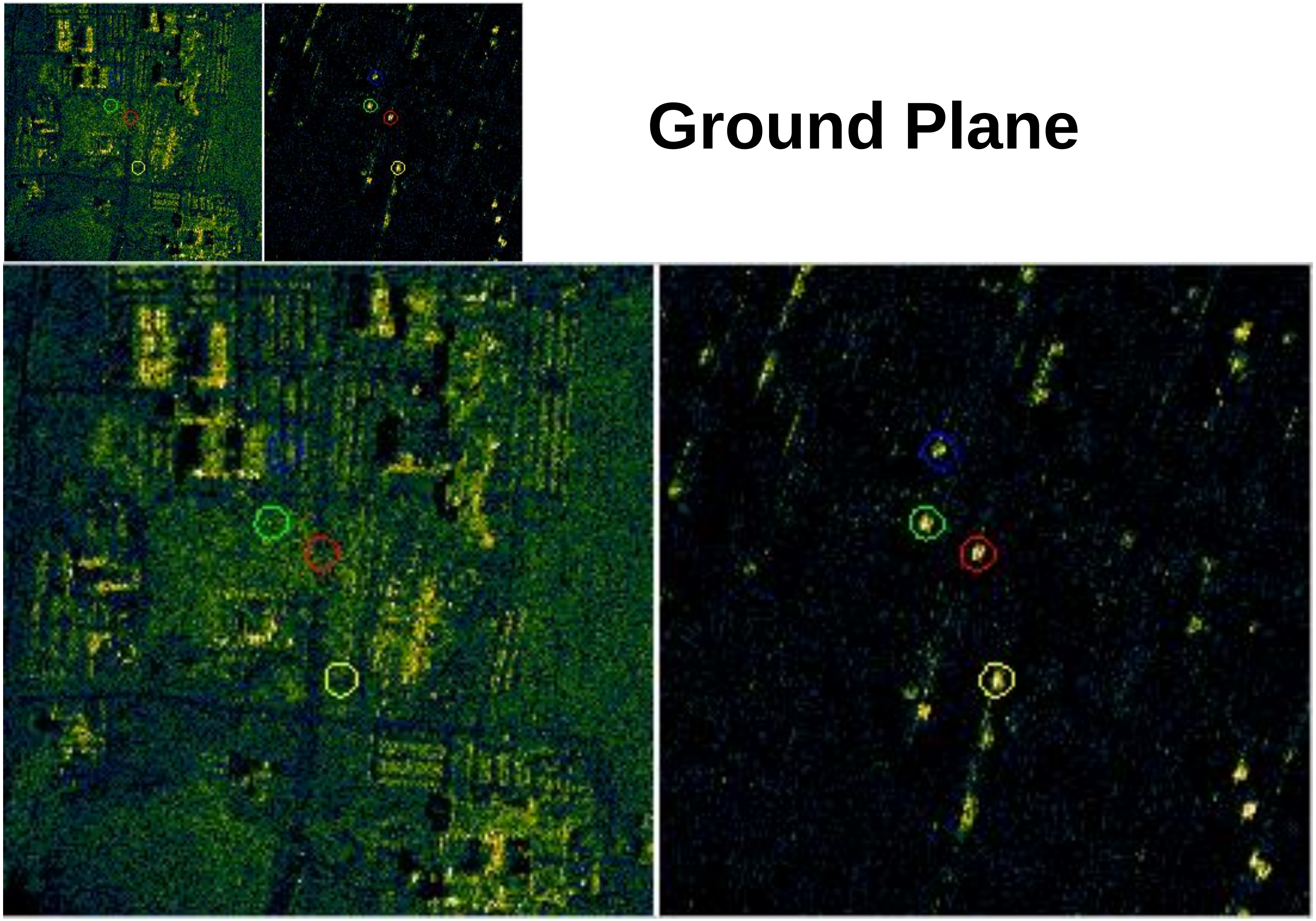

Ground Plane

4. Ground Plane Geolocation

- Moving target coordinates at zero slow-time $\tau = 0$ of a subaperture:

$$\left(X_{\text{target}}^{(\ell)}, Y_{\text{target}}^{(\ell)}, Z_{\text{target}}^{(\ell)} \right)$$

- 3D velocity of moving target (is assumed to be a constant within a subaperture but may vary from one subaperture to another):

$$\left(v_{x\text{target}}^{(\ell)}, v_{y\text{target}}^{(\ell)}, v_{z\text{target}}^{(\ell)} \right)$$

- Distance of moving target from radar (<u>radial-range</u>) as a function of slow-time:

$$R_{\text{radar-target}}^{(\ell)}(\tau)=\begin{bmatrix}\left(X_{\text{radar}}^{(\ell)}+v_{x\text{radar}}^{(\ell)}\tau-X_{\text{target}}^{(\ell)}-v_{x\text{target}}^{(\ell)}\tau\right)^{2}+\\ \left(Y_{\text{radar}}^{(\ell)}+v_{y\text{radar}}^{(\ell)}\tau-Y_{\text{target}}^{(\ell)}-v_{y\text{target}}^{(\ell)}\tau\right)^{2}+\\ \left(Z_{\text{radar}}^{(\ell)}+v_{z\text{radar}}^{(\ell)}\tau-Z_{\text{target}}^{(\ell)}-v_{z\text{target}}^{(\ell)}\tau\right)^{2}\end{bmatrix}^{1/2}$$

- <u>Angular Doppler frequency</u> of moving target as a function of slow-time:

$$\phi_{\text{radar-target}}^{(\ell)}(\tau)$$

where

$$\sin\phi^{(\ell)}_{\text{radar-target}}(\tau) = \frac{\frac{d}{d\tau}R^{(\ell)}_{\text{radar-target}}(\tau)}{v^{(\ell)}_{\text{radar}}}$$

$$= \frac{\begin{bmatrix} \left(v^{(\ell)}_{x\text{radar}} - v^{(\ell)}_{x\text{target}}\right)\left(X^{(\ell)}_{\text{radar}} + v^{(\ell)}_{x\text{radar}}\tau - X^{(\ell)}_{\text{target}} - v^{(\ell)}_{x\text{target}}\tau\right) + \\ \left(v^{(\ell)}_{y\text{radar}} - v^{(\ell)}_{y\text{target}}\right)\left(Y^{(\ell)}_{\text{radar}} + v^{(\ell)}_{y\text{radar}}\tau - Y^{(\ell)}_{\text{target}} - v^{(\ell)}_{y\text{target}}\tau\right) + \\ \left(v^{(\ell)}_{z\text{radar}} - v^{(\ell)}_{z\text{target}}\right)\left(Z^{(\ell)}_{\text{radar}} + v^{(\ell)}_{z\text{radar}}\tau - Z^{(\ell)}_{\text{target}} - v^{(\ell)}_{z\text{target}}\tau\right) \end{bmatrix}}{v^{(\ell)}_{\text{radar}}\, R^{(\ell)}_{\text{radar-target}}(\tau)}$$

- For a subaperture image, moving target signature appears (centered) at

$$\left[\phi^{(\ell)}_{\text{radar-target}}(0), R^{(\ell)}_{\text{radar-target}}(0)\right]$$

Geolocation Using Knowledge of Network of Roads

- Radial-ranges of a moving target for the subapertures could be mapped into the network of roads on the ground plane
- Operator/computer could determine which road is the logical/correct choice by:
  a. Estimating target velocity on a road
  b. Calculating subaperture angular Doppler values from the estimated velocity and other available radar/target parameters
  c. Comparing calculated and actual angular Doppler data

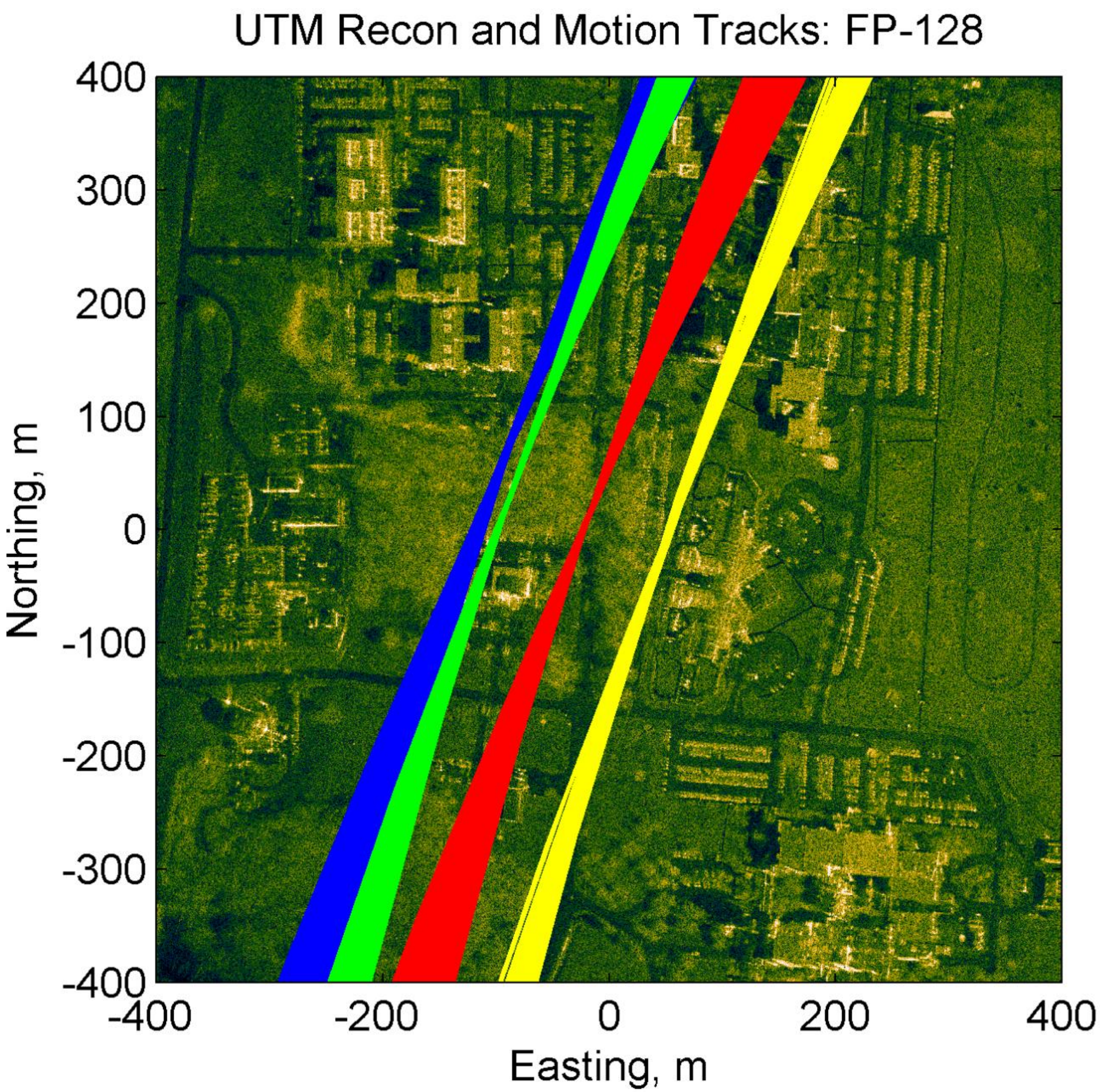
UTM Recon and Motion Tracks: FP-128
400
300
200
100
0
-100
-200
-300
-400
Northing, m
-400
-200
0
200
400
Easting, m

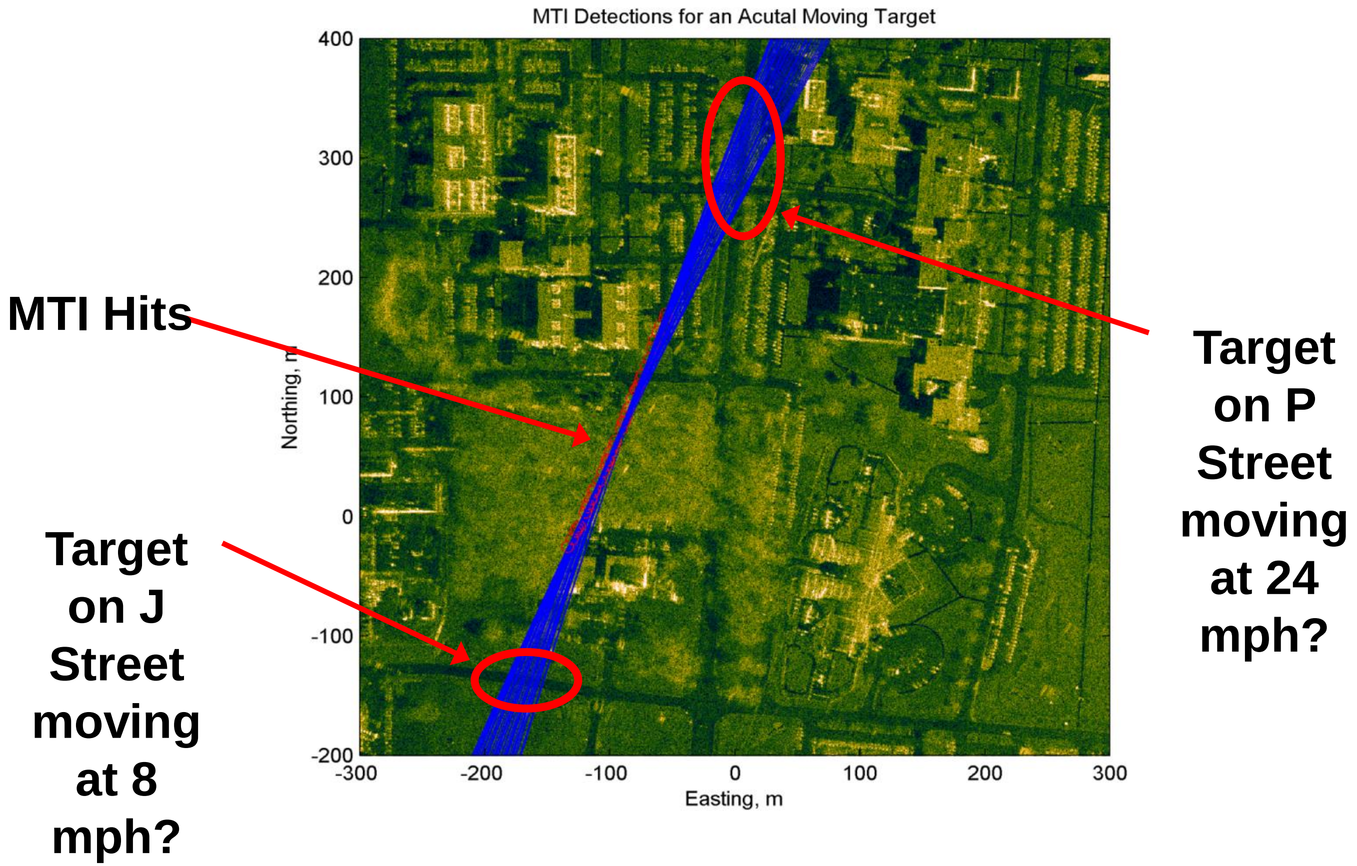

MTI detections for an actual moving target in subapertures 1-40 (red circles), and the lines of constant radial range for the moving target for each subaperture (blue lines)

MTI Results Validation and Target Geolocation via Measured SAR Data & Simulation

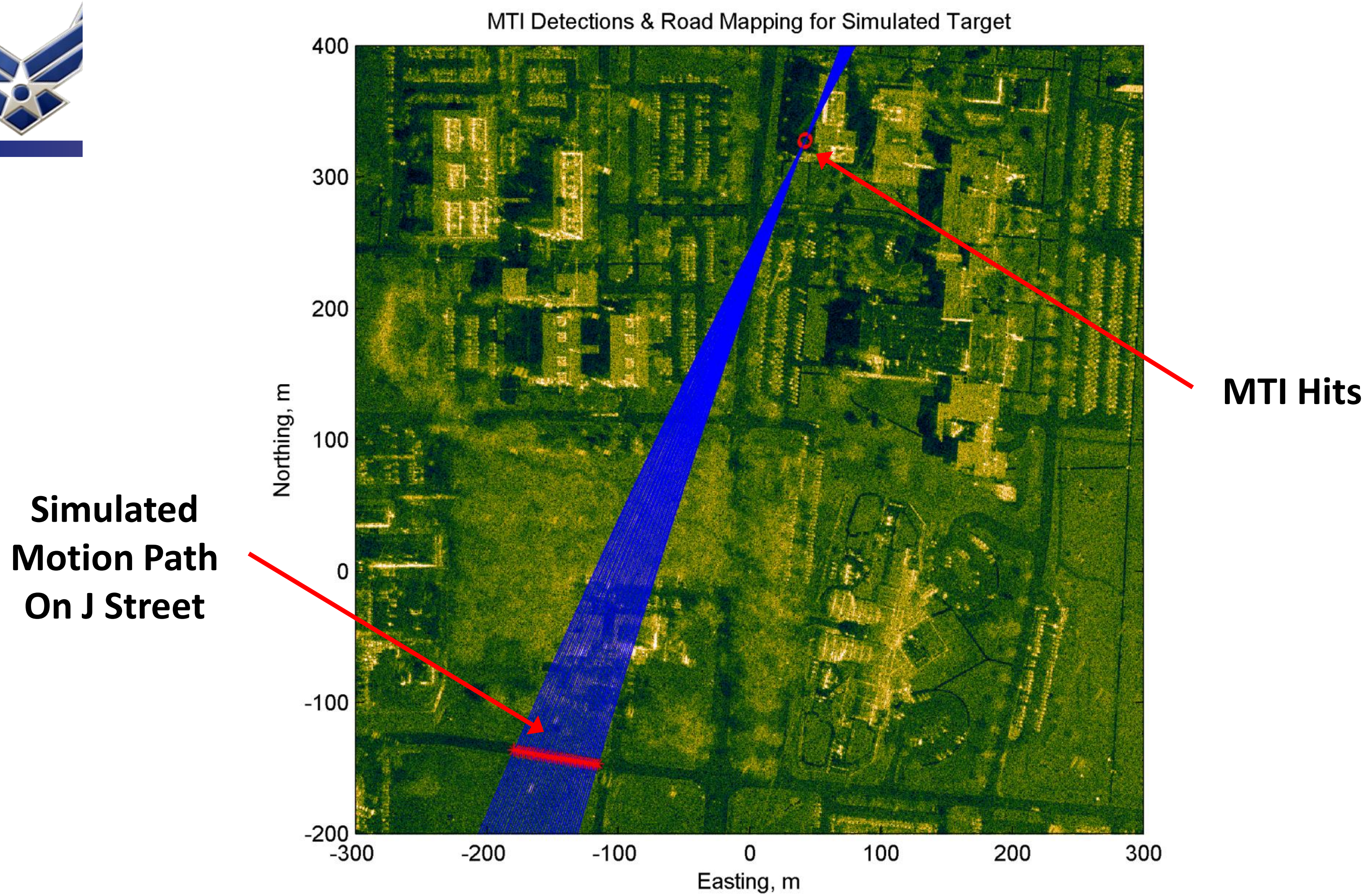

MTI detections for the first simulated moving target (on J Street with speed of 16 mph) in subapertures 1-40 (red circles), the lines of constant radial range for the moving target for each subaperture (blue lines), and the road mapping of the target on J Street (red stars)

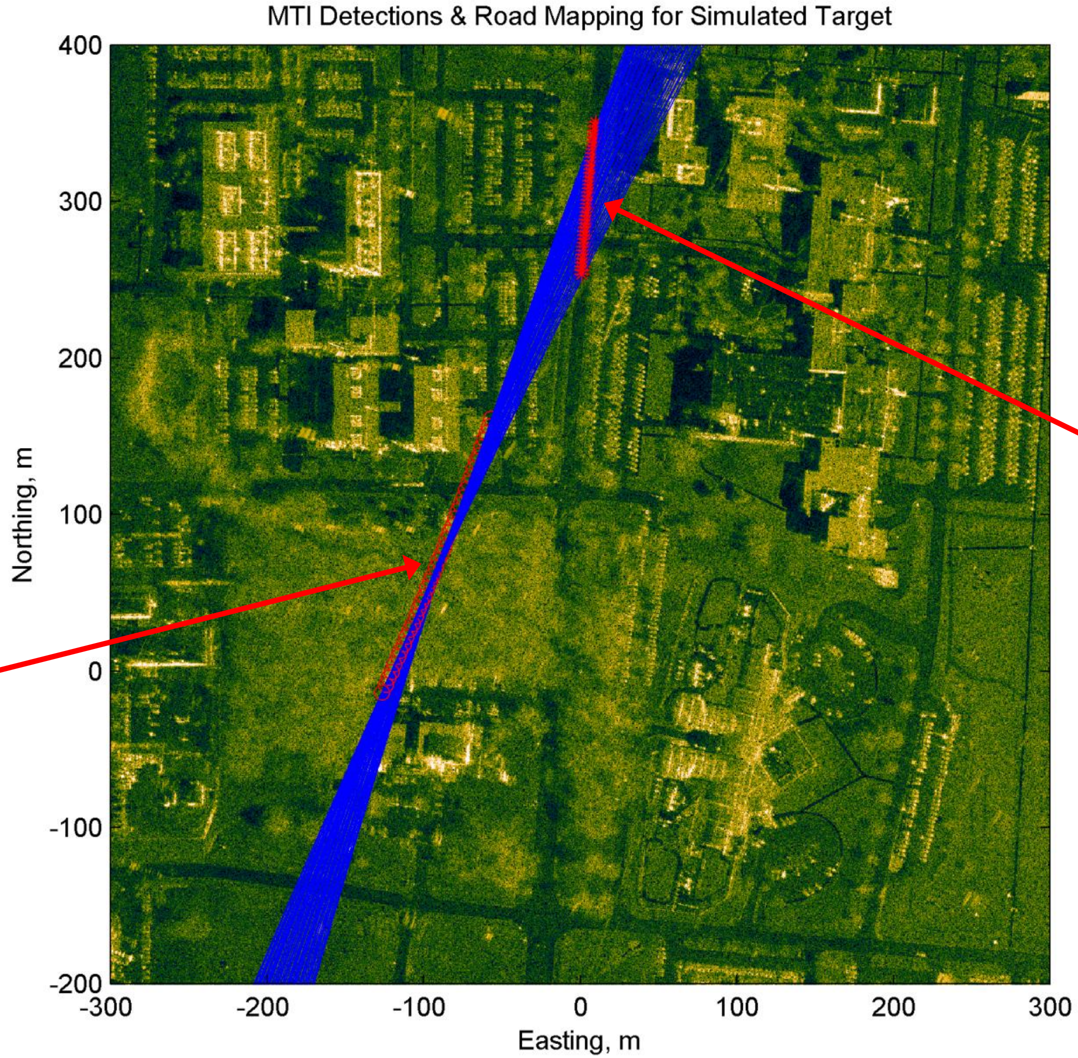

Simulated Motion Path on P Street

MTI Hits

MTI detections for the second simulated moving target (on P Street with speed of 24 mph) in subapertures 1-40 (red circles), the lines of constant radial range for the moving target for each subaperture (blue lines), and the road mapping of the target on P Street (red stars)

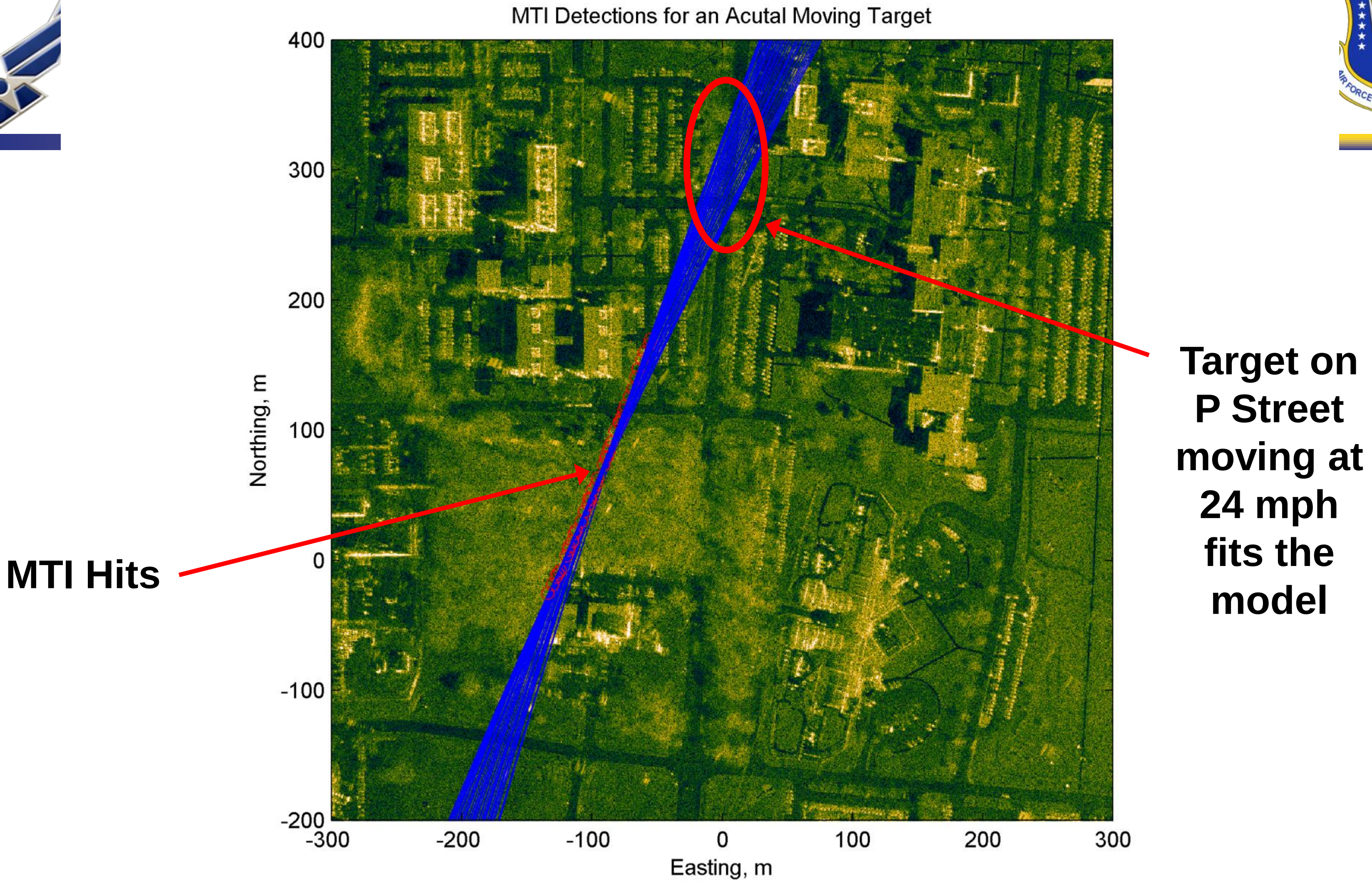

MTI detections for an actual moving target

5. Summary

We Presented:

1. Algorithm to detect multiple moving targets from along-track monopulse SAR data; the algorithm blindly calibrates for various system errors in the two monopulse channels that vary in the image spatial domain.
2. Association, tracking and geolocation algorithms that depend on the signal properties of a moving target SAR signature and the network of roads in the interrogated scene.

Public Release: Document Number 88 ABW-10-1551